DOI:
10.1016/j.molimm.2017.12.018

Document Version
Peer reviewed version

Caspases are key regulators of inflammatory and innate immune responses mediated by TLR3 in vivo.

Abeer Shaalan*[1], Guy Carpenter [1], Gordon Proctor [1]

[1] Mucosal and Salivary Biology Division, Dental Institute, King's College London, Guy's Hospital, Floor 17, Tower Wing, London SE1 9RT, UK

*Corresponding author: abeer.shaalan@kcl.ac.uk.

1. Introduction

Apoptosis has been considered as one of the main factors that may be related to loss of SG secretory function [1]. In fact, death of acinar and ductal cells is considered to be a major mechanism leading to salivary gland dysfunction in patients with Sjögren's syndrome [2] and following irradiation of salivary glands [3]. While apoptosis was classically described as an immunologically silent mode of cell death, several studies have shown that cells and tissues stimulated to undergo apoptosis produce moderate amounts of chemoattractant proteins and cytokines [4], indicating that apoptosis and inflammation are inseparably linked. Recent studies indicate that caspases, the initiators of the apoptotic cell death pathway, are situated at the nexus of vital networks that balance inflammation, antiviral immunity and cell death [5].

Caspases are a family of proteases that have been subdivided functionally into those involved in either apoptosis (caspases-2, -3, -6,-7, -8, -9 and -10 in mammals) or inflammation (caspases-1, -4, -5 and -12 in humans and caspases-1, -11 and -12 in mice) [6]. While the apoptotic caspases function in the initiation and execution of a programmed cell death, inflammatory caspases mediate innate immune responses by cleaving proinflammatory cytokine precursors (for example, pro-IL-1β and pro-IL-18) to initiate inflammation [7].

Emerging studies have shown that caspase inhibition prevents inflammation via preventing T cell activation, Th2 cytokine production and inflammatory cell infiltration [8]. More recent studies showed that pre-treatment with the cell permeable pan-caspase inhibitor z-Val-Ala-Asp (Ome) fluoro-methyl-ketone (z-VAD-fmk), which irreversibly binds to the catalytic site of caspase proteases [9], significantly inhibited the activation of myeloperoxidase (MPO), TNF-α, IL-1β and decreased lung injury in a rat model of severe acute pancreatitis [10]. The role played by all mammalian caspases in the control of inflammatory and immune reactions has recently been thoroughly reviewed [11].

Toll-like receptors (TLRs) are transmembrane pattern recognition receptors, which play key roles in sensing microbial pathogen associated molecular patterns (PAMPs) and mounting an immune response. Indeed, TLRs induce the expression of inflammatory pro-survival factors and cytokines [12], that recruit polymorphonuclear leukocytes (PMNs) to the infection site [13]. TLR3 has been identified as a key sensor for viral dsRNA or its synthetic double stranded (ds)RNA analogue poly (I:C) [14]. In turn, poly (I:C) can elicit apoptosis directly in a TLR3 dependent manner [15]. Despite the recent studies and reviews that propose caspases as the central regulators of apoptosis, inflammation and key effectors of immune responses against microbial infections [5,7,16-19], it is unclear if caspases play an immune regulatory role during acute injury phases *in vivo*. In the current study, we stimulated the TLR3-mediated innate immune response of the C57BL/6 SMGs via the synthetic dsRNA poly (I:C). The induction of a caspase-dependent apoptotic signal in the glandular cells was substantiated as early as nine hours post poly (I:C) intraductal infusion. Moreover, pre-treatment of the mice with z-VAD-fmk, blocked the activated caspases and substantiated their participation in the TLR3-mediated innate immune signalling and cytokine production.

Our results provide, for the first time, evidence that caspases are central in regulating inflammatory cell infiltration and activation of innate immune responses *in vivo* following TLR3 stimulation.

2. Materials and Methods

2.1 Mice

Female C57BL/6 mice weighing 18-21 grams (Harlan Labs Ltd., Loughborough, UK) and aged 10-12 weeks were housed in a temperature-controlled environment under a 12 h light–dark cycle, with free access to food and water. All procedures were approved by the local ethics committee and performed under general anaesthesia under a Home Office license.

2.2 Poly (I:C) injury model

The C57BL/6 mouse SMGs were cannulated as previously performed in rats [20] and mice [21]. Initially, a glass cannula (Supelco, 25715, PA- USA) was stretched over a flame and fitted into a polyethylene tube with 0.28 mm inner diameter. Polyinosinic–polycytidylic acid sodium salt (P1530-25MG, Sigma-Aldrich) was then diluted in 0.9% saline solution to a final concentration of 4mg/ml. Towards consistent, visualised and flawless SMG injection, poly (I:C) was pre-mixed with Trypan blue (T8154-100ML-Sigma- Aldrich) prior to injection. Eighty micrograms of poly (I:C) in 20 µls were loaded into a 0.3 ml syringe (6134900, VWR International). For recovery experiments, mice were anaesthetised intraperitoneally (i.p) with 0.1 ml of combined 5 mg Ketamine/1 mg Xylazine. Under a stereomicroscope, the glass cannula was inserted into Wharton's duct and poly (I:C) was injected slowly and constantly into the left SMG (Fig. 1A). The same volume of the vehicle (0.9% saline and Trypan blue) was delivered to the right SMG as a contralateral negative control.

2.3 Assessment of Submandibular Secretory Function

Animals were anaesthetized with 150 µl of Pentobarbital Sodium (Euthatal, Merial) 1 mg/ml (i.p.), followed by endotracheal intubation. Each submandibular duct was exposed by dissection from the ventral surface through the mylohyoid muscle. Individual submandibular ducts were cut and saliva was collected using polyethylene tubes connected to insulin syringes (Fig. 1B). Saliva collection proceeded for 5 min following onset of secretion after stimulation with pilocarpine (0.5mg/kg i.p.). Following collection into pre-weighed Eppendorf tubes, the tubes were re-weighed, the volume of saliva was calculated as 1mg = 1µl saliva and results were expressed as µL saliva/min.

2.4 Z-VAD-fmk and apoptosis inhibition model

Cell-permeable z-VAD-fmk (BD Pharmingen™, 550377) was dissolved in DMSO, aliquoted and stored at −80°C, and then diluted as needed in PBS for experiments. Mice were pre-treated intraperitoneally with z-VAD-fmk (10mg/kg), 30 minutes prior to intraductal injection with poly (I:C) [22]. In the current study, this group will be referred to as z-VAD-fmk+PIC. The contralateral submandibular gland was injected with the vehicle (0.9% saline and Trypan blue). Tissues were excised and saliva was collected 9 hrs following poly (I:C) intraductal injection.

2.5 TLR3/dsRNA complex inhibitor model

The TLR3/dsRNA complex inhibitor ((R)-2-(3-Chloro-6-fluorobenzo [b] thiophene-2 -carboxamido)-3-phenylpropanoic acid, Calbiochem Merck Millipore, 614310) was used to competitively disrupt poly (I:C) binding to TLR3 [28]. The inhibitor was dissolved in DMSO and diluted in PBS. 1mg/mouse of the inhibitor was intraperitoneally injected into mice [23]. At the same time, 4µg/µl poly (I:C) was combined to 50 ng TLR3/dsRNA and 20 µl of this solution was loaded in a 0.3 ml syringe. Mice were anaesthetised as previously

mentioned and poly (I:C)-TLR3/dsRNA inhibitor were injected slowly and consistently into the SMG. In the current study, this group will be referred to as TLR3-I+PIC. The contralateral SMG was injected with the vehicle (0.9% saline, Trypan blue and 50 ng TLR3/dsRNA complex inhibitor). Tissues were excised and saliva was collected 9 hrs following poly (I:C) intraductal injection.

2.6 Histopathologic Examination

Harvested SMGs were fixed in 10% neutral buffer formalin, processed and embedded in paraffin for long term storage. Poly (I:C) induced histomorphometric changes and immune cell infiltration were examined using conventional H&E stain and contrasted versus the saline injected control glands.

2.7 Immunohistochemical Analysis

Three µm tissue sections were deparaffinized, rehydrated, and unmasked in a single step using Trilogy™ (Cell Marque, Rocklin, CA, 920P-06). To block endogenous peroxidase activity and non-specific background staining sections were incubated in 3% hydrogen peroxide solution for 20-30 minutes. To block all epitopes on the tissue samples and prevent nonspecific antibody binding, sections were incubated with 1% BSA in 1X TBS, pH7.6 for 5 minutes. Primary antibody (Table 1) was applied at the appropriate working dilution overnight at 4°C followed by secondary antibody (Table 1) which was incubated for 60 mins at room temperature. Colour was developed for 5 mins in DAB solution (Pierce™ 34002) and slides were counterstained in Mayer haematoxylin and DPX-mounted for light microscopy.

Table 1 Antibodies used in immunohistochemical analysis

Antibody	Source & Catalogue Number	Working Dilution
anti-dsRNA	SCICONS Budapest, Hungary, J2-1511	1:1500
Cleaved caspase-3	R&D Systems, MAB835	1:280
MPO	BosterBio, USA, PB9057	1:1000
Interleukin 6 (IL-6)	Abcam, Ltd, ab83339	1:900
iNOS	Novus Biologicals, USA, NB300-605	1:700
Polyclonal Goat Anti-Rabbit Immunoglobulins-HRP	Dako, P0448	1:200
Polyclonal Goat Anti-Mouse Immunoglobulins- HRP	Dako, P0447	1:100

2.8 Western Blotting

Tissues stored in RNAlater® were retrieved, homogenized in cell lysis buffer (AA-LYS-10 ml- RayBiotech, Inc., Norcross, GA) plus protease inhibitor cocktail (1:10 dilution, Calbiochem, UK) using a FastPrep™ tissue homogenizer (MP Biomedicals Santa Ana, CA). Protein concentration was measured using the Qubit® protein assay kit (Q33211, Invitrogen™, UK) and Qubit® 3.0 Fluorometer (Q33216, Invitrogen™, UK) and a total of 15-20 µg /lane of the different lysates were separated by SDS-PAGE on a 4-12% Novex polyacrylamide gel (Invitrogen, UK). Electro-transfer of proteins was done for 1 hour to 0.2 µm pore–size nitrocellulose membrane (1620112, Bio-Rad, UK) according to standard protocol (Invitrogen, UK, Paisley), followed by membrane blocking with 5% bovine serum albumin. Membranes were incubated at 4°C overnight with the appropriate antibody (Table 2) in blocking buffer then washed and incubated with the HRP conjugated anti-rabbit secondary antibody in blocking buffer at room temperature for 1 h. For signal development, an Enhanced Chemioluminescence substrate (ECL, GE Healthcare, UK) was prepared following the kit manufacturer's recommendations and applied over the membranes. Excess reagent was flicked and positive and negative protein expression was assessed and captured using ChemiDoc™ MP System (Bio-Rad, UK).

Table 2 Antibodies used in western blot analysis

Antibody	Source & Catalogue Number	Working Dilution
Cleaved Caspase 3	Novus Bio, NB100-56113	1:5000
Cleaved Caspase 8 (Asp387) XP®	Cell Signalling Technology, 8592	1:1000
iNOS	Novus Biologicals, USA, NB300-605	1:1000
IL-1β	Boster, PA1351	1:3000
B-actin	Sigma, A2228	1 µg/mL
Polyclonal Goat Anti-Rabbit Immunoglobulins-HRP	Dako, P0448	1:2000
Polyclonal Goat Anti-Mouse Immunoglobulins- HRP	Dako, P0447	1:1000

2.9 qRT-PCR Analysis

For qRT-PCR analysis, SMGs stored in RNAlater® (R0901-100ml, Sigma-Aldrich) were homogenized using FastPrep™ tissue homogenizer (MP Biomedicals Santa Ana, CA) and RNeasy® Micro Kit (74004, Qiagen) was used for total RNA extraction. RNA concentration as well as the A260/280 and A260/230 ratios were then measured with the NanoDrop ND-1000 Spectrophotometer (Thermo Fischer Scientific, Nottingham UK). iScript™ cDNA Synthesis kit (170-8890, Bio-Rad) was used to reverse transcribe 100 ng of extracted RNA. qPCR reactions (10 µl/well) were prepared by adding SsoAdvanced ™ Universal SYBR Green Supermix (172-5271, Bio-Rad), primers (PrimerDesign™, Ltd.) (Table 3) and cDNA template. Thermal cycling was performed using Corbett RotorGene 6000 System (Qiagen, UK). In all qRT-PCR experiments, relative gene quantification was assessed according to the "Delta Delta CT" (ΔΔCT) [24], where ΔΔCT= [Ct GOI Exp – Ct HKG Exp]-[Ct GOI Cal – Ct HKG Cal]: Ct: cycle threshold, GOI: gene of interest, Exp: poly (I:C)-injected glands, HKG:

housekeeping gene showing the highest stability within each experiment condition, Cal: control glands injected by the vehicle.

Table 3 Primers used in qRT-PCR assessment of gene expression

Gene	Accession Number
TLR3	NM_126166
Mx1 (Mx dynamin-like GTPase 1)	NM_010846
ISG-15 (ISG15 ubiquitin-like modifier)	NM_015783
IL 6	NM_031168
IL 1β	NM_008361
HPRT (Hypoxanthine guanine phosphoribosyl transferase)	NM_013556
GAPDH (glyceraldehyde-3-phosphate dehydrogenase)	NM_008084

2.10 PCR Array of Mouse Toll-Like Receptor Signaling Pathway

To analyse the signalling pathway downstream of TLR3 ligation in SMGs from z-VAD-fmk treated and non-treated animals, the mouse RT² Profiler Toll-Like Receptor (TLR) signaling pathway array was used. RNA was extracted as previously mentioned and 800 ng was reverse transcribed using the RT² First Strand Kit (330401, Qiagen), according to the manufacturer's protocol. Twenty µl of the PCR reaction mix (Table 4) was added to individual wells of the RT² Profiler PCR array format R (PAMM-018ZR, Qiagen) and the thermal cycler was set according to http://www.SABiosciences.com/pcrarrayprotocolfiles.php.

Table 4 qRT-PCR reaction mix

2x RT2 SYBR Green ROX FAST Mastermix (330520, Qiagen)	1150 µl
cDNA synthesis reaction	102 µl
RNase-free water	1048 µl
Total Volume	2300 µl

A threshold value above the background signal was chosen and the CT values for the run samples were extracted to an excel sheet and analysed using the web-based PCR Array Data Analysis Software available at www.SABiosciences.com/pcrarraydataanalysis.php. Altered expression was assessed by comparing poly (I:C) treated glands with their contralateral vehicle-injected control glands, from mice treated and non-treated with z-VAD-fmk.

2.11 Digital image analysis of cleaved caspase-3 and MPO-immunopositive cells

In each tested group, fifteen random high magnification fields (five from three independent experiments) were captured and colour images of 640 × 480 pixel resolution were then analysed by semi-quantitative digitalized image analysis using ImageJ, NIH ® [25]. Briefly, images were transformed by threshold mode to locate the positive immunostained area, then converted to 8-bit images in grey scale. Subsequently, the area percentage of

positive immunostaining was calculated by the area fraction command within measuring mode, which was expressed as the percentage of red pixels/SMG tissue section.

2.12 Statistical analysis

Results were shown as mean ± SEM (standard error of means). Statistical significance between individual comparisons was determined using Student t-test. For multiple comparisons, one-way ANOVA with Sidak's (selected pairs) pairwise tests were used. In addition, Dunnett test was performed for comparing treatment groups with the control group. The calculations were performed with the statistical software package GraphPad Prism (version 7). P values ≤ 0.05 were considered statistically significant.

3. Results

3.1 Poly (I:C) internalization and TLR3 upregulation.

To visualize poly (I:C) internalization, a dsRNA monoclonal antibody was used to track its fate post retrograde injection into the SMG duct. The vehicle-injected SMGs did not show any dsRNA-positive signal. Conversely, the ducts and acini of the poly (I:C)-injected SMGs showed retention of poly (I:C) up to 24 hrs following its injection (Fig.1C). Next, qRT-PCR was performed and revealed that poly (I:C) induced the transcriptional upregulation of TLR3 in the SMGs. Immunohistochemical staining was performed in order to identify cell phenotypes expressing the activated receptor. Basally, TLR3 showed intense membranous and cytoplasmic immunostaining in the intercalated ducts. Following poly (I:C) introduction, TLR3 showed immunopositivity in the basolateral membranes of acinar and duct cells with increased numbers of intensely stained intercalated ducts (Fig. 2A).

3.2 z-VAD-fmk blocked casp-8/csp-3 activated signals induced by TLR3 stimulation

Mice were pre-treated with the TLR3/dsRNA complex inhibitor, which competitively inhibits dsRNA binding to TLR3 and immunohistochemistry was performed to explore the role played by TLR3 in caspase activation. A single poly (I:C) dose induced an extremely significant increase in the percentage of glandular epithelial cells expressing the apoptotic marker: cleaved caspase-3, compared to the vehicle injected control and the TLR3-inhibited glands ($p<0.0001$) (Fig. 2B). In another set of experiments, mice were pre-treated with 10 mg/kg z-VAD-fmk intraperitoneally, 30 minutes prior to intraductal minfusion of poly (I:C). Subsequently, SMGs were harvested and analysed by western blot to confirm blockade of the TLR-3-triggered apoptotic signal. Results obtained from these experiments confirmed that z-VAD-fmk pre-treatment interfered with expression levels of the TLR3-activated subunits of caspase-8/-3 in the poly (I:C)-injected glands (Fig. 3A). In addition, immunohistochemistry, showed downregulated expression of cleaved caspase 3 in the SMGs of the z-VAD-fmk treated animals, compared to those which received poly (I:C) only (Fig. 3B).

3.3 z-VAD-fmk inhibited infiltration of TLR-3-recruited, MPO-positive, acute inflammatory cells

H&E sections from SMGs of the control, poly (I:C)-injected, TLR-3 blocked and z-VAD-treated mice were microscopically examined and revealed that the poly (I:C)-infected glands from both the z-VAD treated and TLR-3-inhibited mice were inflammation- and oedema-free; two hallmark features of the glands injected with poly (I:C) alone (Fig. 4). Next, the anti-inflammatory effect of z-VAD in the poly (I:C) infected glands was verified by immunolabelling tissues with the acute inflammatory marker: MPO (expressed in lysosomes of monocytes and azurophilic granules of neutrophils) [26] and comparing the results to those in the TLR3/dsRNA blockade model. Immunohistochemistry similarly confirmed the H&E results, whereby the SMGs from the poly (I:C) treated mice displayed many MPO positive immune cells, which were absent from the z-VAD- or TLR3-inhibitor-treated mice. (Fig .4).

3.4 Effect of z-VAD-fmk on pilocarpine stimulated saliva secretion

To rule out induction of necroptotic cell death, which is coupled to caspase inhibition [17], the viability of the secretory parenchymal cells was assessed by exploring the functional response of the SMGs to pilocarpine stimulation. Blockade of active caspases using the z-VAD-fmk inhibitor preserved SMG secretory capacity, which had clearly deteriorated 9 hrs post intraductal infusion of poly (I:C). Similar functional protection was conferred by competitively blocking TLR3 (Fig. 5).

3.5 Pan caspase inhibition interfered with transcriptional activation of TLR-related and interferon (IFN) stimulated genes

The mouse RT2 Profiler™ TLR PCR array of 84 TLR-related innate immune adaptor and effector genes was used to broadly analyse SMG response to blockade of the caspase system by z-VAD-fmk. Intriguingly, pre-treating mice with z-VAD-fmk prior to poly (I:C) injection, reduced the expression level of all TLR-related genes, compared to their extensive transcriptional upregulation in the SMGs which received the innate immune stimulant only (Fig. 6A). In addition, specific primers for interferon-responsive genes were used to confirm this novel, negative feedback mechanism executed by caspase inhibition with z-VAD-fmk (Fig. 6B).

Table 5a. Fold change in the expression of mRNA of TLR-related genes, 6 hrs following poly (I:C) injection. mRNA expression was assessed using an RT² Profiler Toll-Like Receptor (TLR) signaling pathway array.

Layout	1	2	3	4	5	6	7	8	9	10	11	12
A	Agfg1	Btk	Casp8	Ccl2	Cd14	Cd80	Cd86	Cebpb	Chuk	Clec4e	Csf2	Csf3
	7.75	3.59	11.84	119.02	28.94	8.78	33.59	-1.12	15.08	55.91	10.7	22.86
B	Cxcl10	Eif2ak2	Elk1	Fadd	Fos	Hmgb1	Hras	Hspa1a	Hspd1	Ifnb1	Ifng	Ikbkb
	522.76	8	1.84	2.6	5.46	16.51	3.57	19.16	9.85	445.72	37.01	2.53
C	Il10	Il12a	Il1a	Il1b	Il1r1	Il2	Il6	Il6ra	Irak1	Irak2	Irf1	Irf3
	8.2	3.05	82.71	70.03	-1.27	1.38	364.56	2.43	4.72	2.9	16.8	6.02
D	Jun	Lta	Ly86	Ly96	Map2k3	Map2k4	Map3k1	Map3k7	Mapk8	Mapk8ip3	Mapk9	Muc13
	3.56	3.67	5.66	8.78	4.45	3.59	2.22	2.57	3.88	1.38	3.84	12.04
E	Myd88	Nfkb1	Nfkb2	Nfkbia	Nfkbib	Nfkbil1	Nfrkb	Nr2c2	Peli1	Pglyrp1	Ppara	Ptgs2
	4.08	17.15	9.13	19.7	3.32	1.24	1.93	5.62	7.16	18.83	-1.27	8.43
F	Rel	Rela	Ripk2	Tbk1	Ticam1	Ticam2	Tirap	Tlr1	Tlr2	Tlr3	Tlr4	Tlr5
	11.55	4.99	41.36	9.71	1.09	1.39	2.52	10.37	12.34	75.06	3.61	1.27
G	Tlr6	Tlr7	Tlr8	Tlr9	Tnf	Tnfaip3	Tnfrsf1a	Tollip	Tradd	Traf6	Ube2n	Ube2v1
	9.32	4.07	3.29	2.32	10.2	23.43	1.82	1.9	8.31	2.69	6.77	11.27

Table 5b Fold change in the expression of mRNA of TLR-related genes 6 hrs following z-VAD-fmk pre-treatment and poly (I:C) injection. mRNA expression was assessed using an RT² Profiler Toll-Like Receptor (TLR) signaling pathway array.

Layout	1	2	3	4	5	6	7	8	9	10	11	12
A	Agfg1	Btk	Casp8	Ccl2	Cd14	Cd80	Cd86	Cebpb	Chuk	Clec4e	Csf2	Csf3
	1.2	1.27	1.48	4.03	2.17	1.48	2.33	-1.01	1.54	8.94	-1.34	18.51
B	Cxcl10	Eif2ak2	Elk1	Fadd	Fos	Hmgb1	Hras	Hspa1a	Hspd1	Ifnb1	Ifng	Ikbkb
	3.78	1.1	1.12	-2.04	1.13	1.26	1.06	1.82	-1.71	5.19	2.2	-1.07
C	Il10	Il12a	Il1a	Il1b	Il1r1	Il2	Il6	Il6ra	Irak1	Irak2	Irf1	Irf3
	2.7	1.53	4.2	23.59	1.01	-1.02	4.58	-1.34	-1.08	-1.13	-1.05	1.11
D	Jun	Lta	Ly86	Ly96	Map2k3	Map2k4	Map3k1	Map3k7	Mapk8	Mapk8ip3	Mapk9	Muc13
	-1.05	1.12	-1.12	2.13	1.06	1.02	-6.63	-1.31	-1.07	-1.32	-1.72	1.29
E	Myd88	Nfkb1	Nfkb2	Nfkbia	Nfkbib	Nfkbil1	Nfrkb	Nr2c2	Peli1	Pglyrp1	Ppara	Ptgs2
	-1.62	1.55	1	-1.02	2.62	1.09	-1.24	1.02	1.06	3.05	-1.73	2.19
F	Rel	Rela	Ripk2	Tbk1	Ticam1	Ticam2	Tirap	Tlr1	Tlr2	Tlr3	Tlr4	Tlr5
	-1.3	1.08	-1.18	-1.9	1.12	1.01	-1.22	-3.72	1.13	1.04	1	-2.03
G	Tlr6	Tlr7	Tlr8	Tlr9	Tnf	Tnfaip3	Tnfrsf1a	Tollip	Tradd	Traf6	Ube2n	Ube2v1
	1.03	-1.76	-1.72	-1.22	3.13	2	-1.55	1.08	1.25	2.24	1.13	1.01

3.6 Caspases are central in regulating the expression of TLR-3-induced pro-inflammatory cytokines

To further define the immune regulatory functions of caspases, we investigated their potential contribution to cytokine production in response to TLR-3 stimulation. SMGs from the TLR3-inhibited and z-VAD-fmk-treated mice exhibited a dramatic decline in the transcriptional activation of the pleotropic cytokines, IL-6 and IL-1β compared to the vehicle injected control glands (Fig. 7A & B). In addition, protein levels of the activated IL-1β isoform (Fig. 7B) and inducible nitric oxide synthase (iNOS) were greatly diminished in parenchymal cells, following ductal injection with poly (I:C) (Fig. 7C).

4. Discussion

The current study provides *in vivo* evidence that caspases regulate the TLR3-activated innate immune response. This conclusion is consistent with the important role played by caspases in coordinating and integrating signals that result not only in apoptosis but also inflammation and immune regulation [27]. Previous studies demonstrated that multiple, systemic injections of poly (I:C) into Sjögren's syndrome-prone, NZB/WF1 mice, resulted in loss of glandular function [28,29]. The TLR3-stimulant in the current model was locally injected into the SMGs to avoid systemic delivery, which is more likely to dilute the poly (I:C) and minimize the chance of its efficient exposure to salivary parenchymal cells. Moreover, the model presented herein, is unique in demonstrating the direct influence of innate immune activation on the SMG tissues and functional responses, ruling out possible extraneous impacts arising either from systemic delivery or autoimmune susceptibility of mice. The cannulation technique established, enabled the development of a reliable and reproducible mouse model, whereby intraductal conveyance of poly (I:C) pre-mixed with Trypan blue allowed consistently successful infusion and delivery of the same amount of inflammagen into the SMGs (even when other drugs such as TLR3/dsRNA inhibitor and z-VAD-fmk, were used). Parenchymal exposure to poly (I:C) and its efficient internalization into the SMG ductal and acinar cells were verified using the J2 monoclonal antibody which specifically recognizes dsRNA of more than 40 base pairs in length [30]. The J2 antibody positively stained acinar and ductal cells which internalized the poly (I:C) and revealed that parenchymal cells retain the inflammagen up to 24 hrs post inoculation.

The involvement of TLR3 in dsRNA-triggered apoptosis has previously been demonstrated by RNA interference [15,31]. Upon ligand recognition, TLR3 recruits the adaptor protein TRIF, which then interacts with the receptor interacting protein 1 (RIP1), a serine/threonine kinase that not only enhances survival through NF-κB and MAPK activation, but also promotes apoptosis by recruiting FADD and by activating caspase-8 [32]. Activated caspase-8 cleaves and activates caspase-3, which then executes the apoptotic program [33]. Intraductal infusion of the poly (I:C) into the SMGs prompted transcriptional upregulation of TLR3, which triggered the expression of activated forms of caspase-8 and caspase-3. Cleaved caspase-3-positive duct and acinar cells were observed as early as 9 hrs after poly (I:C) administration and were significantly decreased in the mice treated with the pan caspase inhibitor z-VAD-fmk. Surprisingly, systemic injection of z-VAD-fmk before challenging the SMG innate immune response, interfered with acute inflammatory cell infiltration and protected the SMG secretory machinery from the poly (I:C)-induced loss of function. z-VAD-fmk has shown therapeutic efficacy in many diseases including neurogenic pulmonary edema [34], muscle ischemia-reperfusion injury [35] and allergic lung inflammation [8].

Caspases are closely inter-connected with cytokines and cytokine receptors, in that some caspases are essential for cytokine maturation (i.e. activation) and secretion. Caspase-1 cleaves pro-IL-1β and pro-IL-18 to the mature cytokine forms [36]. In addition, caspase-3 is involved in the processing of pro-IL-16 to the mature cytokine [37]. It has been previously shown that z-VAD-fmk inhibition of caspase-3 led to the down-regulation of JNK/SAPK and NF-kB, which were required for LPS-induced iNOS expression and NO production [38]. Moreover, caspase-8 has been reported to directly cleave pro IL-1β into its mature, active form following TLR3/TLR4 stimulation [39], in addition to its direct activation of the inflammatory caspase-1, in an inflammasome-independent manner [40]. IL-1β can recruit a cascade of events downstream of the IL-1R complex, resulting in the activation of important signalling proteins, such as mitogen-activated kinases (JNK, p38, ERK1/2), as well as transcription factors, including NFκB (p65 and p50 subunits) and c-Jun (a subunit of AP-1), which control expression of a number of inflammatory and catabolic genes [41]. Whether TLR3 engages caspases for maximal cytokine production is not known, but the broad anti-inflammatory effect provided by z-VAD-fmk in the current injury model may have been down to its ability to inhibit caspases that cleave pro-IL-1β into its active form.

In addition to their apoptotic roles, a new paradigm for caspases in non-apoptotic roles has become clear. In the current study, the pan caspase inhibitor, z-VAD-fmk negatively regulated the expression of an array of TLR-related and IFN-stimulated genes. This finding may be due to the pleiotropic role of caspase-8 in the control of gene expression downstream of TLR stimulation [42], via: (i) induction of mRNA transcription and promotion of mRNA stability [17], (ii) localization to nuclei, raising the possibility that nuclear caspase-8 might play a role in gene expression [43] and (iii) regulating the activation of the transcription factor NF-κB [42,44-46], which induces the expression of target genes, including cytokines, chemokines, and adhesion molecules [47].

IFNs contribute to immune protection through the induction of cellular antimicrobial programmes and through enhancing immune responses for the efficient termination of infection [48]. However, type-I-IFNs can also be harmful, either by inducing immunosuppressive effects that impede viral control [49] or by triggering inflammation and tissue damage that exacerbate disease [50]. The results from arrays in the present study show very remarkable downregulation of the poly (I:C) induced Ifnb1 from 445 folds to 5 folds, when mice received the pan caspase inhibitor prior to poly (I:C). To confirm this novel and therapeutically significant finding, qRT-PCR was carried out to further analyse the mRNA expression levels of IFN-response genes in poly (I:C) treated SMGs from the z-VAD-fmk treated and non-treated mice. Results from these experiments confirmed the array finding and revealed for the first time that caspase inhibition can potentially control unruly type I IFN-regulated genes. However, the mechanism(s) by which caspases directly or indirectly regulate the IRF-pathway in SMGs has not previously been addressed. Thus, further studies are needed to determine the importance of caspases for IRF signalling in response to TLR agonists *in vivo*.

In conclusion, the current study is the first to demonstrate that the broad-spectrum caspase inhibitor z-VAD-fmk can regulate TLR3-induced gene expression and cytokine production *in vivo*, during the early stages of innate immune activation and inflammation.

Conflict of Interest: The authors declare that they have no conflict of interest.

Funding: This research did not receive any specific grant from funding agencies in the public, commercial, or not-for-profit sectors.

References

1. Hayashi T (2011) Dysfunction of lacrimal and salivary glands in Sjogren's syndrome: nonimmunologic injury in preinflammatory phase and mouse model. J Biomed Biotechnol 2011: 407031.
2. Horai Y, Nakamura H, Nakashima Y, Hayashi T, Kawakami A (2016) Analysis of the downstream mediators of toll-like receptor 3-induced apoptosis in labial salivary glands in patients with Sjogren's syndrome. Mod Rheumatol 26: 99-104.
3. Acauan MD, Figueiredo MA, Cherubini K, Gomes AP, Salum FG (2015) Radiotherapy-induced salivary dysfunction: Structural changes, pathogenetic mechanisms and therapies. Arch Oral Biol 60: 1802-1810.
4. Cullen SP, Henry CM, Kearney CJ, Logue SE, Feoktistova M, et al. (2013) Fas/CD95-induced chemokines can serve as "find-me" signals for apoptotic cells. Mol Cell 49: 1034-1048.
5. Chen H, Ning X, Jiang Z (2017) Caspases control antiviral innate immunity. Cell Mol Immunol 14: 736-747.
6. Cohen GM (1997) Caspases: the executioners of apoptosis. Biochem J 326 (Pt 1): 1-16.
7. Man SM, Kanneganti TD (2016) Converging roles of caspases in inflammasome activation, cell death and innate immunity. Nat Rev Immunol 16: 7-21.
8. Iwata A, Nishio K, Winn RK, Chi EY, Henderson WR, Jr., et al. (2003) A broad-spectrum caspase inhibitor attenuates allergic airway inflammation in murine asthma model. J Immunol 170: 3386-3391.
9. Gregoli PA, Bondurant MC (1999) Function of caspases in regulating apoptosis caused by erythropoietin deprivation in erythroid progenitors. J Cell Physiol 178: 133-143.
10. Liu M, Shi L, Zou X, Zheng X, Zhang F, et al. (2016) Caspase inhibitor zVAD-fmk protects against acute pancreatitis-associated lung injury via inhibiting inflammation and apoptosis. Pancreatology 16: 733-738.
11. Galluzzi L, Lopez-Soto A, Kumar S, Kroemer G (2016) Caspases Connect Cell-Death Signaling to Organismal Homeostasis. Immunity 44: 221-231.
12. Janeway CA, Jr., Medzhitov R (2002) Innate immune recognition. Annu Rev Immunol 20: 197-216.
13. Kumar A, Zhang J, Yu F-SX (2006) Toll-like receptor 3 agonist poly(I:C)-induced antiviral response in human corneal epithelial cells. Immunology 117: 11-21.
14. Blasius AL, Beutler B (2010) Intracellular toll-like receptors. Immunity 32: 305-315.
15. Salaun B, Coste I, Rissoan MC, Lebecque SJ, Renno T (2006) TLR3 can directly trigger apoptosis in human cancer cells. J Immunol 176: 4894-4901.
16. McIntire CR, Yeretssian G, Saleh M (2009) Inflammasomes in infection and inflammation. Apoptosis 14: 522-535.
17. Philip NH, DeLaney A, Peterson LW, Santos-Marrero M, Grier JT, et al. (2016) Activity of Uncleaved Caspase-8 Controls Anti-bacterial Immune Defense and TLR-Induced Cytokine Production Independent of Cell Death. PLoS Pathog 12: e1005910.
18. Uchiyama R, Tsutsui H (2015) Caspases as the key effectors of inflammatory responses against bacterial infection. Arch Immunol Ther Exp (Warsz) 63: 1-13.
19. Sagulenko V, Lawlor KE, Vince JE (2016) New insights into the regulation of innate immunity by caspase-8. Arthritis Res Ther 18: 4.
20. Correia PN, Carpenter GH, Paterson KL, Proctor GB (2010) Inducible nitric oxide synthase increases secretion from inflamed salivary glands. Rheumatology (Oxford) 49: 48-56.
21. Bombardieri M, Barone F, Lucchesi D, Nayar S, van den Berg WB, et al. (2012) Inducible tertiary lymphoid structures, autoimmunity and exocrine dysfunction in a novel model of salivary gland inflammation in C57BL/6 mice(). Journal of immunology (Baltimore, Md : 1950) 189: 3767-3776.
22. Equils O, Moffatt-Blue C, Ishikawa TO, Simmons CF, Ilievski V, et al. (2009) Pretreatment with pancaspase inhibitor (Z-VAD-FMK) delays but does not prevent intraperitoneal heat-killed group B Streptococcus-induced preterm delivery in a pregnant mouse model. Infect Dis Obstet Gynecol 2009: 749432.
23. Takemura N, Kawasaki T, Kunisawa J, Sato S, Lamichhane A, et al. (2014) Blockade of TLR3 protects mice from lethal radiation-induced gastrointestinal syndrome. Nat Commun 5: 3492.
24. Winer J, Jung CKS, Shackel I, Williams PM (1999) Development and Validation of Real-Time Quantitative Reverse Transcriptase–Polymerase Chain Reaction for Monitoring Gene Expression in Cardiac Myocytesin Vitro. Analytical Biochemistry 270: 41-49.
25. Schneider CA, Rasband WS, Eliceiri KW (2012) NIH Image to ImageJ: 25 years of image analysis. Nat Methods 9: 671-675.
26. Klebanoff SJ (2005) Myeloperoxidase: friend and foe. J Leukoc Biol 77: 598-625.
27. Creagh EM (2014) Caspase crosstalk: integration of apoptotic and innate immune signalling pathways. Trends Immunol 35: 631-640.

28. Deshmukh US, Nandula SR, Thimmalapura PR, Scindia YM, Bagavant H (2009) Activation of innate immune responses through Toll-like receptor 3 causes a rapid loss of salivary gland function. J Oral Pathol Med 38: 42-47.
29. Nandula SR, Dey P, Corbin KL, Nunemaker CS, Bagavant H, et al. (2013) Salivary gland hypofunction induced by activation of innate immunity is dependent on type I interferon signaling. J Oral Pathol Med 42: 66-72.
30. Schonborn J, Oberstrass J, Breyel E, Tittgen J, Schumacher J, et al. (1991) Monoclonal antibodies to double-stranded RNA as probes of RNA structure in crude nucleic acid extracts. Nucleic Acids Res 19: 2993-3000.
31. Jego G, Bataille R, Geffroy-Luseau A, Descamps G, Pellat-Deceunynck C (2006) Pathogen-associated molecular patterns are growth and survival factors for human myeloma cells through Toll-like receptors. Leukemia 20: 1130-1137.
32. Han KJ, Su X, Xu LG, Bin LH, Zhang J, et al. (2004) Mechanisms of the TRIF-induced interferon-stimulated response element and NF-kappaB activation and apoptosis pathways. J Biol Chem 279: 15652-15661.
33. Aliprantis AO, Yang RB, Weiss DS, Godowski P, Zychlinsky A (2000) The apoptotic signaling pathway activated by Toll-like receptor-2. Embo j 19: 3325-3336.
34. Suzuki H, Sozen T, Hasegawa Y, Chen W, Zhang JH (2009) Caspase-1 inhibitor prevents neurogenic pulmonary edema after subarachnoid hemorrhage in mice. Stroke. United States. pp. 3872-3875.
35. Iwata A, Harlan JM, Vedder NB, Winn RK (2002) The caspase inhibitor z-VAD is more effective than CD18 adhesion blockade in reducing muscle ischemia-reperfusion injury: implication for clinical trials. Blood 100: 2077-2080.
36. Fantuzzi G, Dinarello CA (1999) Interleukin-18 and interleukin-1 beta: two cytokine substrates for ICE (caspase-1). J Clin Immunol 19: 1-11.
37. Zhang Y, Center DM, Wu DM, Cruikshank WW, Yuan J, et al. (1998) Processing and activation of pro-interleukin-16 by caspase-3. J Biol Chem 273: 1144-1149.
38. Chakravortty D, Kato Y, Sugiyama T, Koide N, Mu MM, et al. (2001) Inhibition of caspase 3 abrogates lipopolysaccharide-induced nitric oxide production by preventing activation of NF-kappaB and c-Jun NH2-terminal kinase/stress-activated protein kinase in RAW 264.7 murine macrophage cells. Infect Immun 69: 1315-1321.
39. Maelfait J, Vercammen E, Janssens S, Schotte P, Haegman M, et al. (2008) Stimulation of Toll-like receptor 3 and 4 induces interleukin-1beta maturation by caspase-8. J Exp Med 205: 1967-1973.
40. Philip NH, Dillon CP, Snyder AG, Fitzgerald P, Wynosky-Dolfi MA, et al. (2014) Caspase-8 mediates caspase-1 processing and innate immune defense in response to bacterial blockade of NF-kappaB and MAPK signaling. Proc Natl Acad Sci U S A 111: 7385-7390.
41. Risbud MV, Shapiro IM (2014) Role of cytokines in intervertebral disc degeneration: pain and disc content. Nat Rev Rheumatol 10: 44-56.
42. Moen SH, Westhrin M, Zahoor M, Norgaard NN, Hella H, et al. (2016) Caspase-8 regulates the expression of pro- and anti-inflammatory cytokines in human bone marrow-derived mesenchymal stromal cells. Immun Inflamm Dis 4: 327-337.
43. Besnault-Mascard L, Leprince C, Auffredou MT, Meunier B, Bourgeade MF, et al. (2005) Caspase-8 sumoylation is associated with nuclear localization. Oncogene 24: 3268-3273.
44. Lemmers B, Salmena L, Bidere N, Su H, Matysiak-Zablocki E, et al. (2007) Essential role for caspase-8 in Toll-like receptors and NFkappaB signaling. J Biol Chem 282: 7416-7423.
45. Weng D, Marty-Roix R, Ganesan S, Proulx MK, Vladimer GI, et al. (2014) Caspase-8 and RIP kinases regulate bacteria-induced innate immune responses and cell death. Proc Natl Acad Sci U S A 111: 7391-7396.
46. Su H, Bidere N, Zheng L, Cubre A, Sakai K, et al. (2005) Requirement for caspase-8 in NF-kappaB activation by antigen receptor. Science 307: 1465-1468.
47. Traenckner EB, Pahl HL, Henkel T, Schmidt KN, Wilk S, et al. (1995) Phosphorylation of human I kappa B-alpha on serines 32 and 36 controls I kappa B-alpha proteolysis and NF-kappa B activation in response to diverse stimuli. Embo j 14: 2876-2883.
48. McNab F, Mayer-Barber K, Sher A, Wack A, O'Garra A (2015) Type I interferons in infectious disease. Nat Rev Immunol 15: 87-103.
49. Biron CA (2001) Interferons alpha and beta as immune regulators--a new look. Immunity 14: 661-664.
50. Davidson S, Crotta S, McCabe TM, Wack A (2014) Pathogenic potential of interferon αβ in acute influenza infection. 5: 3864.

Figure Legends

Fig 1 Poly (I:C) retrograde ductal injection and saliva collection. **A**: Microscopic depiction of pre-fabricated glass cannula inserted into the sublingual papilla of Wharton's duct for poly (I:C) delivery. **B**: Extraoral saliva collection. Mylohyoid muscle slits enclosed the accumulated saliva, that was withdrawn using polyethylene tubes attached to 0.3 ml syringe. **C:** Negative J2 immunolabelling of poly (I:C) in the vehicle-injected glands (V-C). Six hrs post poly (I:C) injection, the synthetic dsRNA was immunolocalized in the perinuclear areas of the duct cells (green outline and arrows) as well as the basolateral membranes of acinar cells (yellow outline and arrows), whereas after 24 hrs, more dispersed and less immunostaining intensity of poly (I:C) was detected in duct cells as well as acinar cells. Original magnification= 40x.

Fig 2 A: Expression of TLR3 in the SMGs. **Left:** Transcriptional upregulation of mTLR3 in the SMGs, 6 hrs post poly (I:C) injection (6h P-PIC). Data represent means ± SEM (n=3). ****p≤0.0001. V-C: vehicle injected control, HPRT: Hypoxanthine guanine phosphoribosyl transferase (housekeeping gene). **Right:** immunoexpression of the dsRNA sensor. ***V-C:*** basal TLR3 expression in intercalated duct cells (arrow). ***P-PIC:*** after poly (I:C) injection, intense membranous and cytoplasmic positivity of intercalated ducts (yellow arrow) as well as mild basolateral staining of the acinar cells (red arrow). **B:** Immunohistochemical expression of cleaved caspase-3 in the ductal (yellow arrow) and acinar (red arrow) cells, 9 hrs P-PIC. Original magnification= 40x. Image analysis demonstrated that poly (I:C) remarkably induced the apoptotic signal in the SMGs in a TLR3 dependent manner. ns: non-significant p>0.05, ****p<0.0001.

Fig 3 A: Western blot representation of caspase-8 and caspase-3 in the SMGs, 9 hrs P-PIC. Poly (I:C) induced caspase activation in a TLR-3-dependent manner. The protein products of caspase-8 and caspase-3 extracted from three independent vehicle (V-C), poly (I:C) (P-PIC) injected, TLR3-blocked (TLR3-I+PIC) and caspase-inhibited (z-VAD-fmk+PIC) SMGs, were measured by Western blot analysis. Bars represent the fold change in protein levels of activated subunits of caspase-8 and caspase-3, on the basis of β-actin and indicate mean values ± SEM (n = 3 in each group). ns: non-significant, ***P<0.001, ****p<0.0001 significant differences between the V-C and tested groups. **B:** Immunohistochemical expression of cleaved caspase-3 in SMGs from z-VAD-fmk-treated and non-treated mice, 9 hrs P-PIC introduction.

Fig 4: H&E and MPO-immunostained sections demonstrating control and poly (I:C)-injected SMGs. The SMGs which received the carrier vehicle (V-C) showed normal histology in the form of packed acini and patent ducts. By 9 hrs, the poly (I:C)-infected glands (P-PIC) exhibited widespread infiltration of MPO-positive immune cells in extended stromal spaces, obscuring interlobular ducts and invading inter-acinar tissues. Very few MPO-positive immune cells were detected in the TLR3-blocked (TLR3-I+PIC) and z-VAD-fmk-treated animals (z-VAD-fmk+PIC). Original magnification H&E=25x, MPO=40x. Bars represent area percentage of MPO positive cells in the SMG tissue sections, n=3 for each tested group. ns: non-significant p>0.05, ****p<0.0001.

Fig 5: Mean ± SEM salivary flow rates of the control (V-C), poly (I:C)-injected (P-PIC), TLR3-blocked (TLR3-I+PIC) and caspase-inhibited ((z-VAD-fmk+PIC)) SMGs. Representative results from 3 independent experiments. A single i.p injection of z-VAD-fmk, 30 mins prior to poly (I:C) retrograde infusion, preserved saliva secretion**,** compared to its complete loss, 9 hrs post infusion of the inflammagen, in the non-treated animals**.** Similar functional protection was seen in the glands from mice which received the TLR3/dsRNA competitive blocker.

Fig 6 A: Scatter plot depicting the RT2 profiler PCR array of Toll Like Receptor pathway genes. The plot gives an overview of the expression of 84 genes in the control versus poly (I:C)-injected SMGs, 6 hrs P-PIC, from mice treated and non-treated with z-VAD-fmk. The central line indicates unchanged gene expression; boundaries represent the two-fold regulation cut-off. In red, up-regulated genes; in green, down regulated genes; and in black, genes not altered. Blocking the apoptotic signal in the SMGs by pre-treating mice with z-VAD-fmk, reduced the expression level of all TLR-related genes, compared to the extensive transcriptional upregulation seen in the SMGs which received poly (I:C) only. One representative experiment presented from three biological repeats. **B:** mRNA relative expression of the IFN-response genes: Mx1 and ISG15. Note the extremely significant (p<0.0001)

decrease in the expression of the tested genes in the glands from z-VAD-fmk-treated animals. Data represents means ± SEM (n=3). ns: non-significant $p>0.05$, *$P\leq0.05$, ****$p\leq0.0001$.

Fig 7 A and B (Left): To further confirm the array results, mRNA expression of the pro-inflammatory cytokines IL-6 and IL-1β were investigated in the SMGs from mice non-treated and treated either with z-VAD-fmk or TLR3/dsRNA complex inhibitor. The pleiotropic cytokines IL-6 and IL-1 β demonstrated transcriptional downregulation in response to pan caspase inhibition, ****$p<0.0001$. (**Right):** immunohistochemical representation of IL-6 expression in the SMGs confirmed the inhibiting effect of caspases and TLR3 blockades on the parenchymally-expressed cytokine (acinar cells: yellow arrow and duct cells: red arrow). Original magnification = 40x. Western blot analysis of cleaved IL-1β in SMGs from control (V-C) and poly (I:C) (P-PIC) injected groups, with TLR3/dsRNA complex inhibitor or the caspase inhibitor z-VAD-fmk. Poly (I:C) induced the expression of the mature IL-1β isoform in the SMGs, which was efficiently abrogated by TLR3 blockade or pan caspase inhibition. The data are representative of results from three independent experiments. **C:** Immunohistochemistry and western blot revealed that pan caspase inhibition remarkably diminished the TLR-3-induced acinar iNOS overproduction (arrows). Bars represent the fold change of iNOS protein levels on the basis of β-actin and indicate mean values ± SEM (n = 3 in each group). Western blot data are representative of results from three independent experiments. ns: non-significant $p>0.05$, *$P < 0.05$, significant differences between the V-C and tested groups.

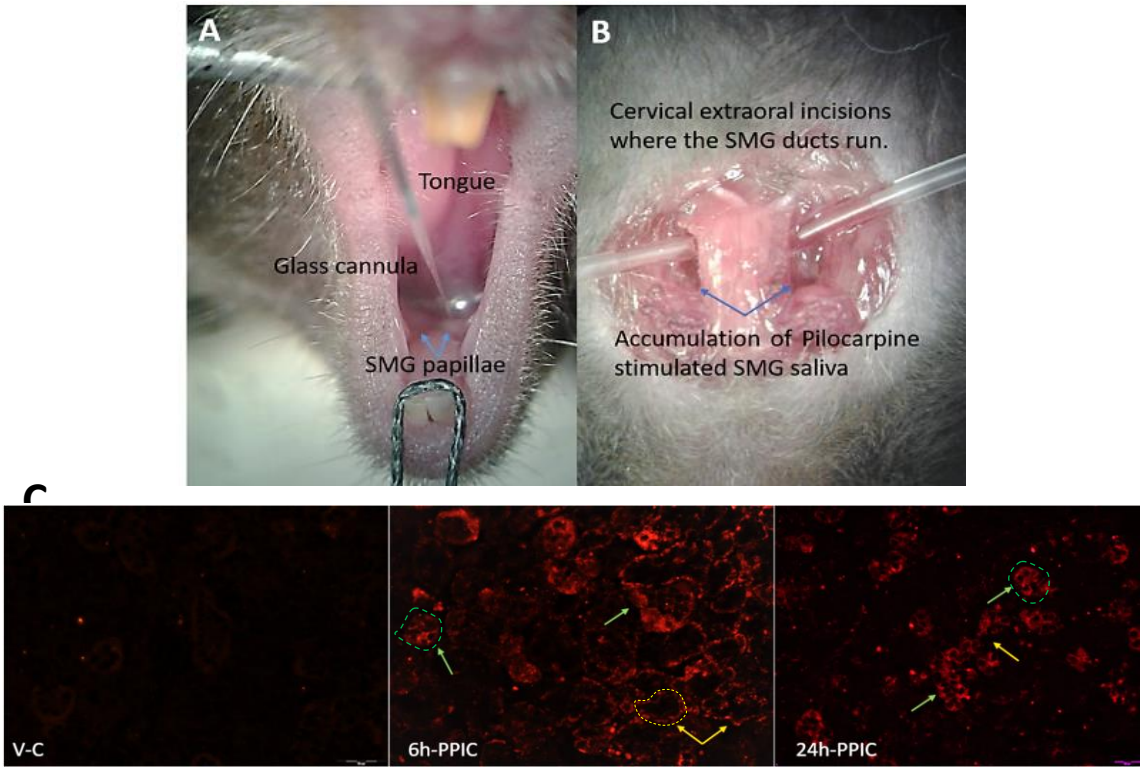
A
Tongue
Glass cannula
SMG papillae
B
Cervical extraoral incisions
where the SMG ducts run.
Accumulation of Pilocarpine
stimulated SMG saliva
C
V-C
6h-PPIC
24h-PPIC

Figure 1.

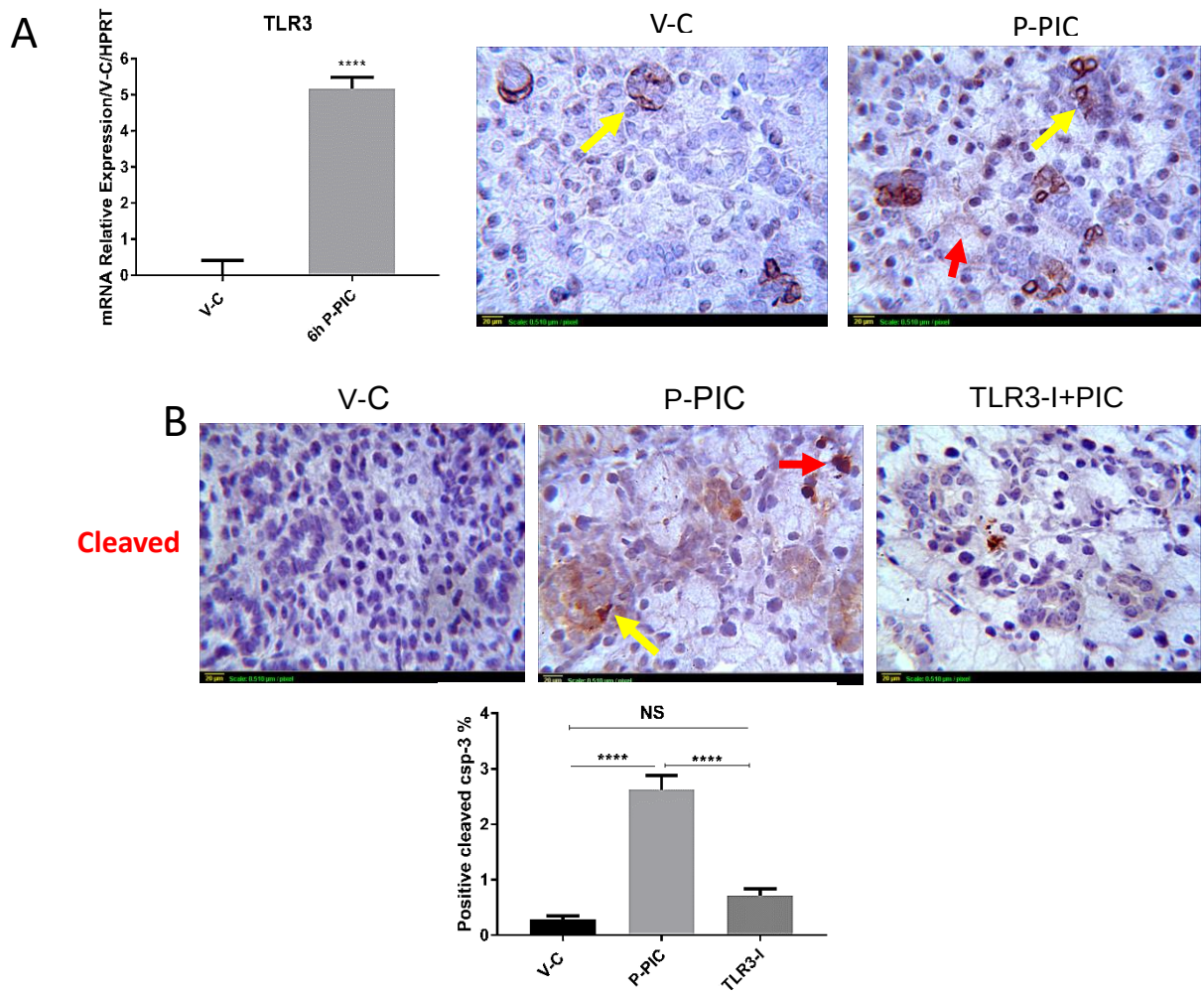
A
TLR3
mRNA Relative Expression/V-C/HPRT
****
V-C
6h P-PIC
V-C
P-PIC
B
V-C
P-PIC
TLR3-I+PIC
Cleaved
NS
****
****
Positive cleaved csp-3 %
V-C
P-PIC
TLR3-I

Figure 2.

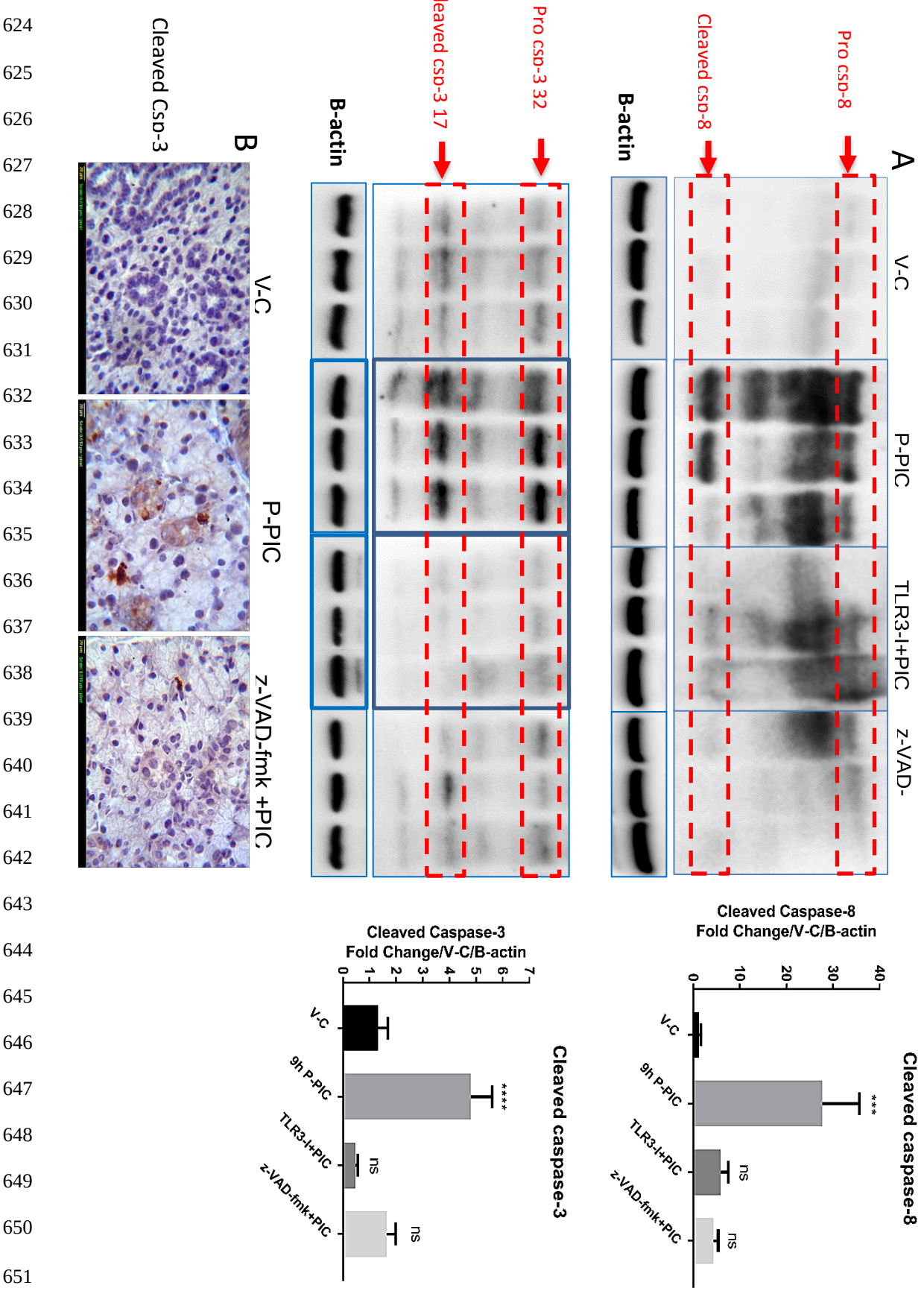
A
Pro csp-8
Cleaved csp-8
B-actin
V-C
P-PIC
TLR3-I+PIC
z-VAD-
Pro csp-3 32
Cleaved csp-3 17
B-actin
Cleaved Caspase-8
Fold Change/V-C/B-actin
Cleaved caspase-8
V-C
9h P-PIC
TLR3-I+PIC
z-VAD-fmk+PIC
***
ns
ns
Cleaved Caspase-3
Fold Change/V-C/B-actin
Cleaved caspase-3
V-C
9h P-PIC
TLR3-I+PIC
z-VAD-fmk+PIC
****
ns
ns
B
Cleaved Csp-3
V-C
P-PIC
z-VAD-fmk +PIC

Figure 3

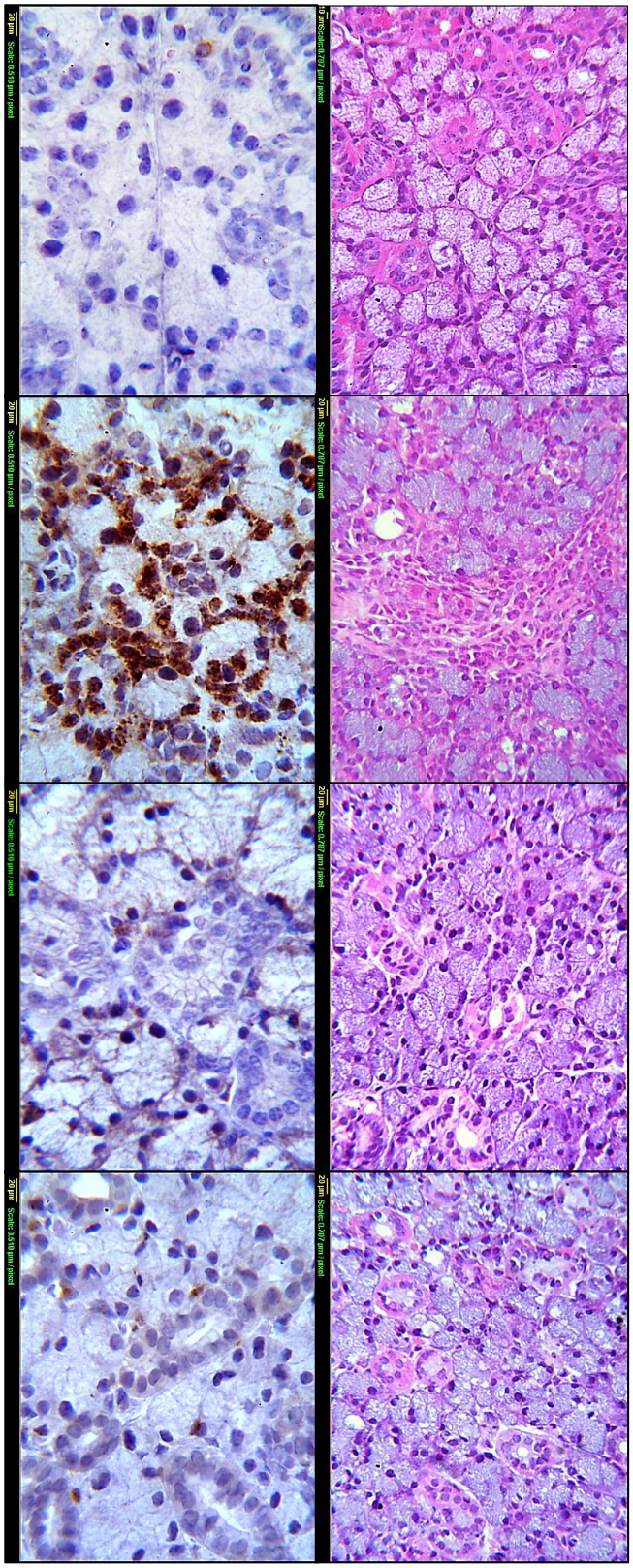
H&E
MP
V-C
P-PIC
TLR3-I+PIC
z-VAD-
Positive MPO %
0
5
10
15
V-C
P-PIC
TLR3-I+PIC
z-VAD-fmk+PIC
****
****
NS
****

Figure 4

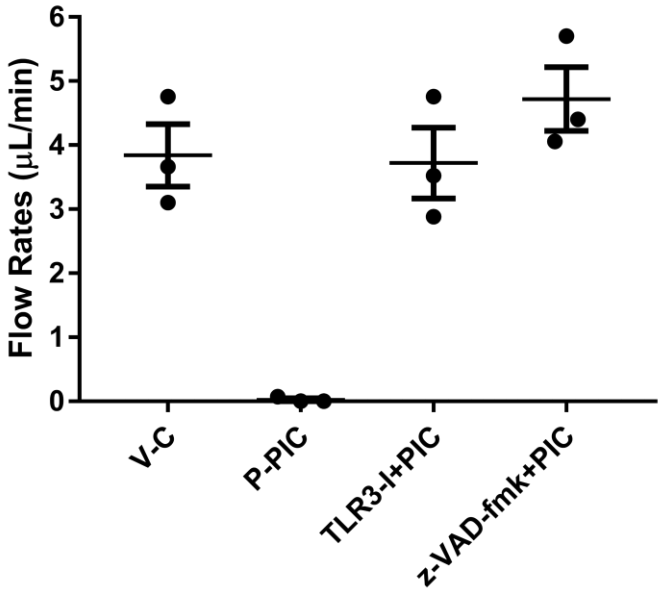

684

685

686 Figure 5

687

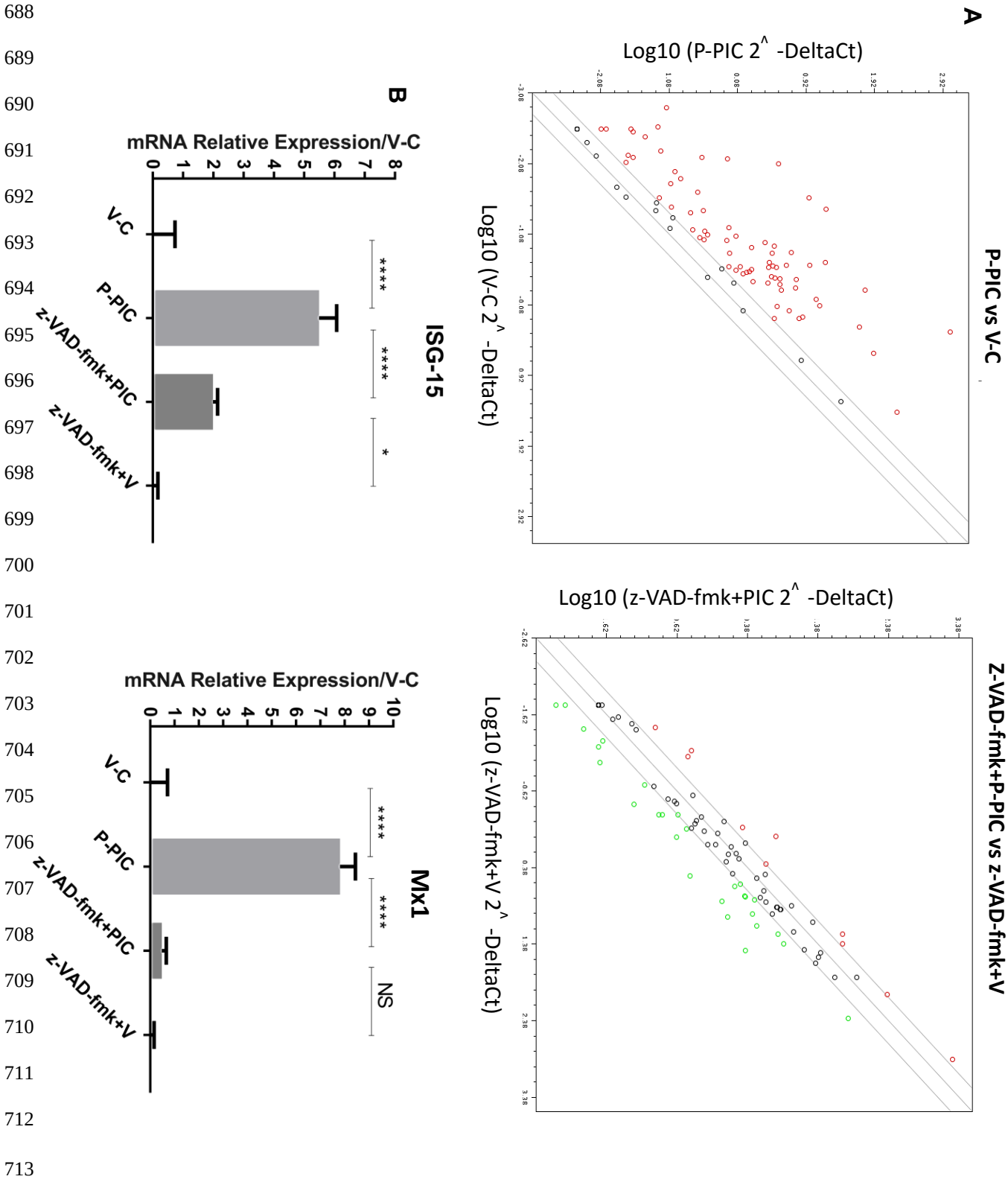
A
P-PIC vs V-C
Log10 (P-PIC 2^ -DeltaCt)
Log10 (V-C 2^ -DeltaCt)
Z-VAD-fmk+P-PIC vs z-VAD-fmk+V
Log10 (z-VAD-fmk+PIC 2^ -DeltaCt)
Log10 (z-VAD-fmk+V 2^ -DeltaCt)
B
ISG-15
mRNA Relative Expression/V-C
V-C
P-PIC
z-VAD-fmk+PIC
z-VAD-fmk+V
****
****
*
Mx1
mRNA Relative Expression/V-C
V-C
P-PIC
z-VAD-fmk+PIC
z-VAD-fmk+V
****
****
NS

Figure 6

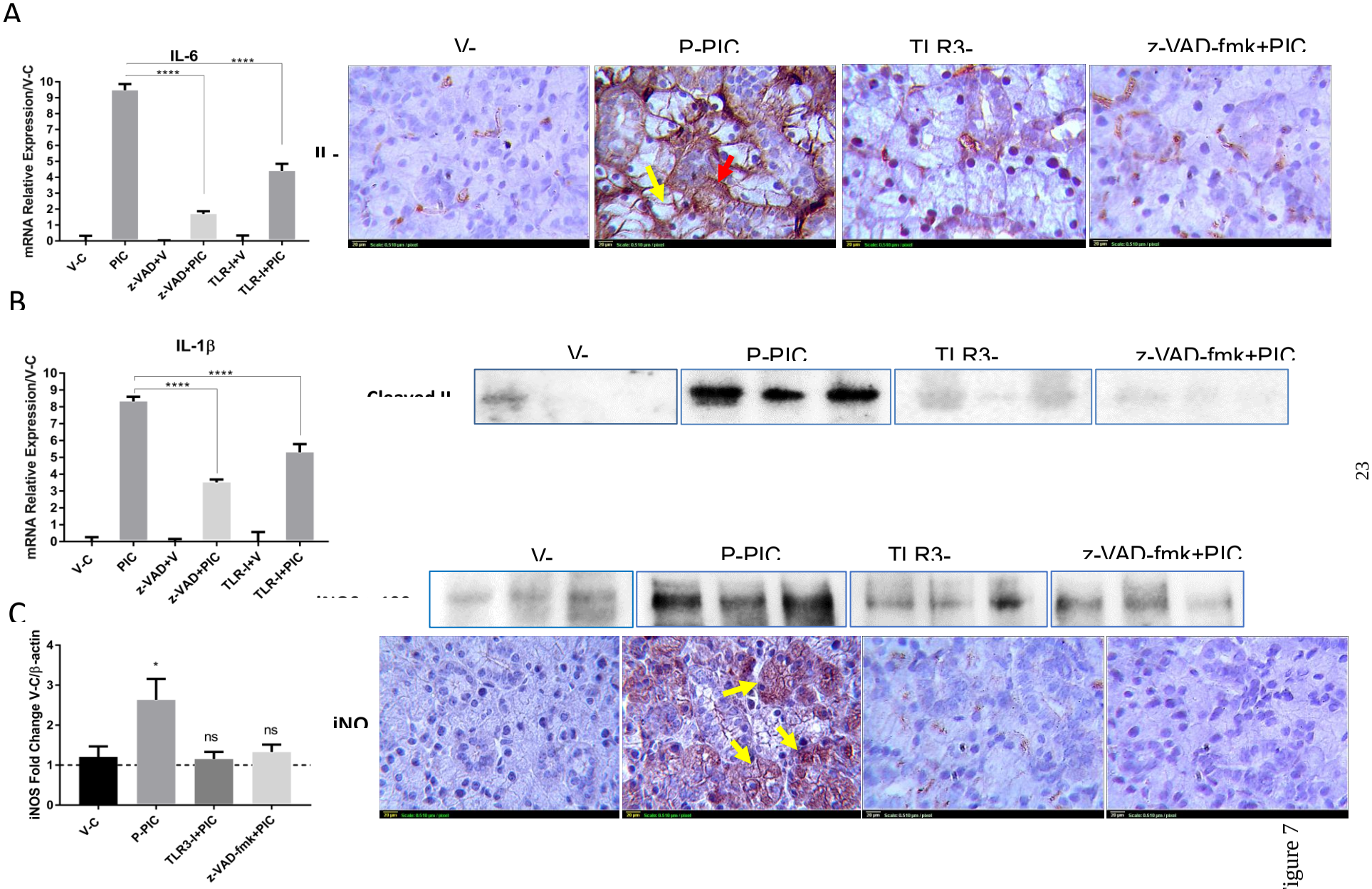
A
IL-6
mRNA Relative Expression/V-C
****
****
V-C
PIC
z-VAD+V
z-VAD+PIC
TLR-I+V
TLR-I+PIC
V-
P-PIC
TLR3-
z-VAD-fmk+PIC
B
IL-1β
mRNA Relative Expression/V-C
****
****
V-C
PIC
z-VAD+V
z-VAD+PIC
TLR-I+V
TLR-I+PIC
V-
P-PIC
TLR3-
z-VAD-fmk+PIC
C
iNOS Fold Change V-C/β-actin
*
ns
ns
V-C
P-PIC
TLR3-I+PIC
z-VAD-fmk+PIC

Figure 7